Six-jet production as a probe of triple parton scattering at the LHC
Summer Student Project

Marina Maneyro
David d'Enterria (Supervisor)
EP Department, Geneva, CERN

1 Introduction

Increasing collision energies at the experimental level can enable more complete insights on the nature of hadrons such as the proton. This is due, for example, to the larger parton densities perceived when probing hadrons at greater energy. Within this context, it has become increasingly relevant to study processes characterized by the production of high transverse momentum particles through several independent parton interactions. These multiparton interactions (MPIs) can be utilized as tools to shed light on the partonic makeup of hadrons. This project focused on the production of six jets in pp and pPb collisions as a vehicle for the study of Triple Parton Scattering processes.

2 Theoretical Background

A simple approach to calculating cross sections for Multiple Parton Interactions is to use products of Single Parton cross sections which could independently produce the outgoing particles. In a pp collision, the probability of Double Parton Scattering (DPS) production of particles X_1 and X_2 can be expressed by multiplying the probabilities of producing X_1 and X_2 in independent Single Parton Scattering (SPS) events. Observables for SPS can be obtained directly from perturbative Quantum Chromodynamics calculations. Normalizing this product to ensure correct units in the result leads to:

$$\sigma_{\rm DPS}^{pp\to X_1\,X_2} = \left(\frac{m}{2}\right) \frac{\sigma_{\rm SPS}^{pp\to X_1}\,\sigma_{\rm SPS}^{pp\to X_2}}{\sigma_{\rm eff,DPS}}, \tag{1}$$

where $m = 1\ (2)$ if $X_1 = X_2$ ($X_1 \neq X_2$) is a combinatorial factor to avoid double counting the same process. The effective cross section $\sigma_{\rm eff,DPS}$ introduced by the normalization can be determined in a purely geometric approach via

$$\sigma_{\rm eff,DPS} = \left[\int d^2b\,T^2(\mathbf{b})\right]^{-1}, \tag{2}$$

where $T(\mathbf{b}) = \int \rho(\mathbf{b_1})\rho(\mathbf{b_1}-\mathbf{b})d^2b_1$ (with $\int d^2bT(\mathbf{b}) = 1$) is the pp transverse overlap function at collision impact parameter b which depends on the transverse parton density of the proton $\rho(\mathbf{b_i})$.

The value of $\sigma_{\rm eff,DPS}$ has been estimated from different geometrical models, which fail to account for parton correlations within protons. This leads to discrepancies with experimental values from the LHC and Tevatron. For the purposes of this project, the experimental value of $\sigma_{\rm eff,DPS} \approx 15$ mb was utilized.

The cross sections for the TPS processes of interested can likewise be expressed from the product of independent SPS cross sections. For the production of particles X_1, X_2 and X_3 in a pp interaction it can be expressed as:

$$\sigma_{\rm TPS}^{pp\to X_1\,X_2\,X_3} = \left(\frac{m}{3!}\right) \frac{\sigma_{\rm SPS}^{pp\to X_1}\,\sigma_{\rm SPS}^{pp\to X_2}\,\sigma_{\rm SPS}^{pp\to X_3}}{\sigma_{\rm eff,TPS}^2}. \tag{3}$$

The combinatorial factor takes values $m = 1$ if $X_1 = X_2 = X_3$, $m = 3$ for the case of two different particles involved (i.e. $X_1 = X_2 \neq X_3$), $m = 6$ if all particles are different.

The effective TPS cross section $\sigma_{\rm eff,TPS}$ can be derived from the pp overlap function, via [1]

$$\sigma_{\rm eff,TPS} = \left[\int d^2b\, T^3(\mathbf{b})\right]^{-1/2} = \kappa\, \sigma_{\rm eff,DPS}, \text{ with } \kappa = (0.82 \pm 0.11), \tag{4}$$

where the numerical value of the κ proportionality factor between effective DPS and TPS cross sections has been obtained studying a large variety of proton transverse parton densities $\rho(\mathbf{b_i})$ and neglecting parton correlations [2].

The study of multiple jet production has been historically one of the experimental approaches to constraint double parton scatterings in high-energy $p\bar{p}$ [3,4] and pp [5,6] collisions. This work presents a new proposal to constrain TPS from the concurrent production of six high-$p_\perp$ jets in pp collisions at 14 TeV. The three generic types of partonic scatterings contributing to the production of the 6-jet final state are shown in Fig. 1. In SPS (leftmost), all six jets are produced by a single pair of interacting partons, whereas two (or three) different pairs of partons produce the final state in DPS (center) and TPS (rightmost), respectively.

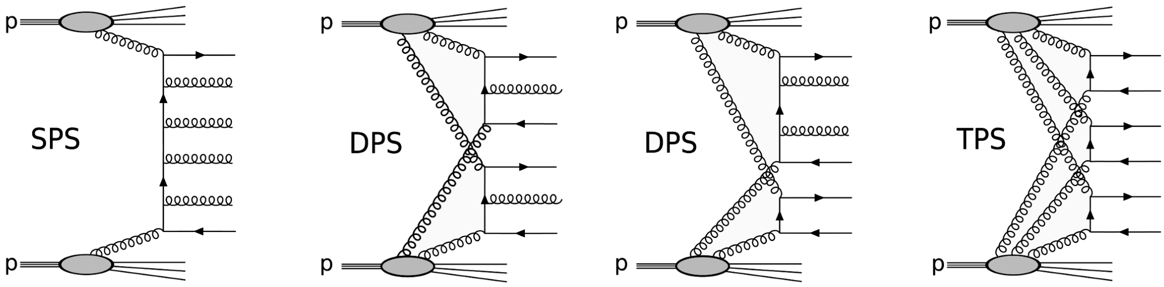

Figure 1: Representative diagrams of SPS (leftmost), DPS (center, with DPS1 (3j+3j) and DPS2 $(4j + 2j)$ processes), and TPS (rightmost) contributions to the production of six jets in pp collisions.

Alongside pp collisions, DPS and TPS cross sections can be obtained for proton-nucleus (pA) interactions. From a theoretical perspective, these results can be calculated from proton-nucleon (pN, for $N = p, n$) SPS cross sections by implementing appropriate scaling procedures. This scaling reflects the parton flux, which now must take into account the amount of nucleons present in the colliding nuclei. Proton-nucleon cross sections are modified according to:

$$\sigma^{\rm SPS}_{\rm pA\to a} = \sigma^{\rm SPS}_{\rm pN\to a} \int d^2b\, T_{\rm pA}(\mathbf{b}) = A \cdot \sigma^{\rm SPS}_{\rm pN\to a}\,. \tag{5}$$

The standard nuclear thickness function $T_{\rm pA}(\mathbf{r})$ is analogous to the transverse overlap function $T(\mathbf{b})$ of the pp case. It is defined by integrating a nuclear density function $\rho_A(\mathbf{r})$ over the proton-nucleus impact parameter, as shown in equation 6. The function needs to be normalized according to scaling factor A.

$$T_{\rm pA}(\mathbf{r}) = \int \rho_A\big(\sqrt{r^2+z^2}\big)\, dz, \quad \text{with} \int T_{\rm pA}(\mathbf{r})\, d^2r = A\,. \tag{6}$$

Enhanced models for DPS cross-sections $\sigma^{\rm DPS}_{\rm pA}$ include two distinct contributions: interactions between partons from the same nucleon (1), and between partons belonging to two different nucleons (2), as shown in Figure 2.

$$\sigma^{\rm DPS}_{\rm pA} = \sigma^{\rm DPS,1}_{\rm pA} + \sigma^{\rm DPS,2}_{\rm pA}\,, \tag{7}$$

The first term is simply obtained by scaling the nucleon level DPS cross sections according to A:

$$\sigma^{\rm DPS,1}_{\rm pA\to ab} = A \cdot \sigma^{\rm DPS}_{\rm pN\to ab}\,. \tag{8}$$

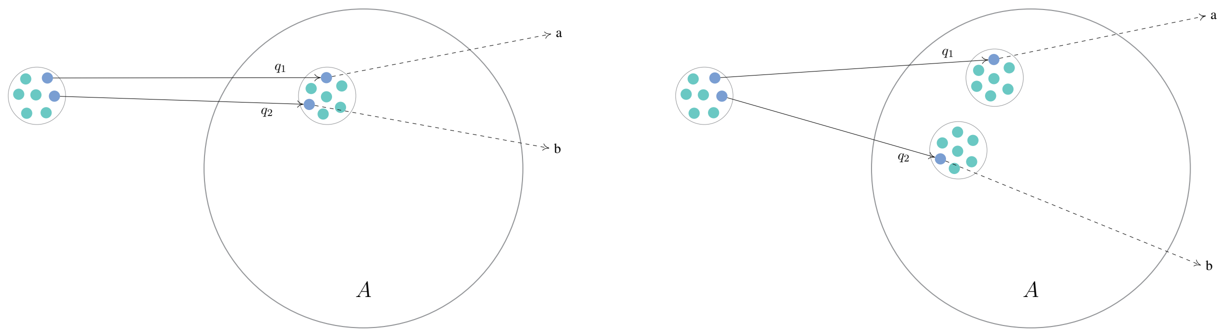

Figure 2: Diagrams representing contributions 1 (Fig. a) and 2 (Fig. b) to DPS pA scattering.

The second contribution depends on $T^2_{\mathrm{pA}}(\mathbf{r})$ as follows:

$$\sigma^{\mathrm{DPS},2}_{\mathrm{pA}\to ab} = \sigma^{\mathrm{DPS}}_{\mathrm{pN}\to ab} \cdot \sigma_{\mathrm{eff,DPS}} \cdot F_{\mathrm{pA}}, \quad \text{with } F_{\mathrm{pA}} = \frac{A-1}{A} \int T^2_{\mathrm{pA}}(\mathbf{r})\, d^2 r\,. \tag{9}$$

The factor $A - 1/A$ in the definition of F_{pA} takes into the account the difference between the total number of nucleon pairs and the number of pairs that are different. The simplest approach to approximate the expression in 9 is to consider a uniform distribution of nucleons within a spherical nucleus, with radius $R_{\mathrm{A}} \propto A^{1/3}$. This work used $A = 208$, for pPb collisions. Then, in the large A limit the value obtained is $F_{\mathrm{pA}} \approx 31.5$ mb^{-1}, which shows good agreement with more sophisticated estimations.

The resulting inclusive DPS cross section for proton-lead collisions can be summarized as:

$$\sigma^{\mathrm{DPS}}_{\mathrm{pA}\to ab} = \left(\frac{m}{2}\right) \frac{\sigma^{\mathrm{SPS}}_{\mathrm{pN}\to a} \cdot \sigma^{\mathrm{SPS}}_{\mathrm{pN}\to b}}{\sigma_{\mathrm{eff,DPS,pA}}}\,, \tag{10}$$

where the new effective cross section introduced includes the dependence in A, the geometry contained in F_{pA} and the pN effective DPS cross section. For the case of a lead nucleus, $\sigma_{\mathrm{eff,DPS,pA}} = 22.5 \pm 2.3$ μb, leading to larger pPb DPS cross sections relative to the pp case.

Obtaining TPS cross sections for the pA case is analogous to the DPS procedure, with the distinction that there are three terms which must be included:

$$\sigma^{\mathrm{TPS}}_{\mathrm{pA}} = \sigma^{\mathrm{TPS},1}_{\mathrm{pA}} + \sigma^{\mathrm{TPS},2}_{\mathrm{pA}} + \sigma^{\mathrm{TPS},3}_{\mathrm{pA}}\,. \tag{11}$$

The first terms represents the interaction between three partons from the proton and three partons from the same nucleon. It is written as the scaling of the pN TPS cross section:

$$\sigma^{\mathrm{TPS},1}_{\mathrm{pA}\to abc} = A \cdot \sigma^{\mathrm{TPS}}_{\mathrm{pN}\to abc}\,. \tag{12}$$

The second contribution involves interactions between partons from two different nucleons in the nucleus, and depends on the square of T_{pA},

$$\sigma^{\mathrm{TPS},2}_{\mathrm{pA}\to abc} = \sigma^{\mathrm{TPS}}_{\mathrm{pN}\to abc} \cdot 3\, \frac{\sigma^2_{\mathrm{eff,TPS}}}{\sigma_{\mathrm{eff,DPS}}}\, F_{\mathrm{pA}}, \tag{13}$$

where F_{pA} takes the form previously defined in equation 9. The third and last contribution represents the interactions with three partons, all coming from different nucleons within the nucleus. This depends on the cube of T_{pA}:

$$\sigma^{\mathrm{TPS},3}_{\mathrm{pA}\to abc} = \sigma^{\mathrm{TPS}}_{\mathrm{pN}\to abc} \cdot \sigma^2_{\mathrm{eff,TPS}} \cdot C_{\mathrm{pA}}, \quad \text{with } C_{\mathrm{pA}} = \frac{(A-1)(A-2)}{A^2} \int d^2 b\, T^3_{\mathrm{pA}}(\mathbf{b})\,, \tag{14}$$

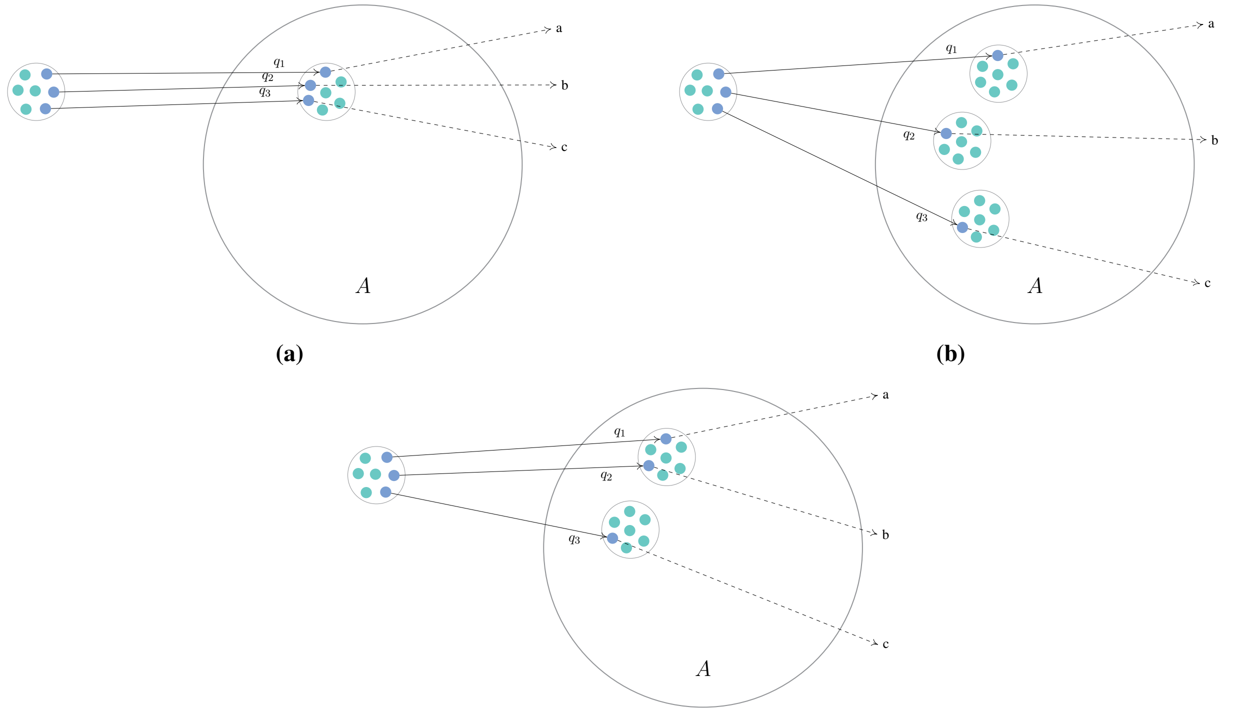

(a) **(b)**

(c)

Figure 3: Diagrams representing contributions 1 (Fig. a), 2 (Fig. b), and 3 (Fig. c) to TPS pA scattering.

Factor $(A-1)(A-2)/A^2$ reflects the difference between the total number of TPS groups and the number of different TPS groups in the nucleus. Considering once again the approximations used for $F_{\rm pA}$, the value obtained for lead nuclei is $C_{\rm pA} \approx 5.1$ mb^{-2}.

The resulting inclusive TPS cross section for pA can be expressed by introducing the TPS effective cross section for the pA case, $\sigma_{\rm eff,TPS,pA}$.

$$\sigma^{\rm TPS}_{{\rm pA}\to abc} = \left(\frac{m}{6}\right) \frac{\sigma^{\rm SPS}_{{\rm pN}\to a} \cdot \sigma^{\rm SPS}_{{\rm pN}\to b} \cdot \sigma^{\rm SPS}_{{\rm pN}\to c}}{\sigma^2_{\rm eff,TPS,pA}} \tag{15}$$

The new effective cross section depends on scaling factor A, geometric quantities $F_{\rm pA}$ and $C_{\rm pA}$, and the TPS effective cross section for pN. In the case of lead, the numerical value is $\sigma_{\rm eff,TPS,pA} = 0.29 \pm 0.04$ mb, taking $\sigma_{\rm eff,TPS} = 12.5 \pm 4.5$ mb.

3 Methodology

Besides gaining familiarity of the theoretical background from the previous section, during this project I obtained different results for the analysis. This included learning to generate collision events using existing Monte Carlo Generation software. This produced numerical values for cross sections, as well as Les Houches event files, which were inputs of the analysis. The jet multiplicities used were $2j$, $3j$, $4j$ $6j$. DPS contributions for $6j$ can be obtained from the equations on the previous section, using $2j$+$4j$ as well as $3j$+$3j$. Meanwhile $6j$ TPS cross sections can be calculated for $2j$+$2j$+$2j$.

For the purpose of this work, it was necessary to implement both Alpgen and Madgraph5_aMC@NLO Monte Carlo generators at 14TeV. The use of MadGraph was vital to take the study to Next-to-Leading-Order precision. However, this generator is not applicable at higher jet multiplicities, such as the $6j$ case that was studied. The generation of $6j$ events was therefore carried out using Alpgen, limited to Leading Order. Thus, it was necessary to check the compatibility of the results from both generators.

One of the theoretical challenges in the study of jet production observable is the choice of an adequate dynamical scale. The standard scale choice utilized by previous studies is $\hat{H}_T/2 = \sum_i p_{T,i}$, where the summation is carried over all outgoing partons in a process. The scale uncertainties as obtained by varying the scale over ($\hat{H}_T$,$\hat{H}_T/2$, $\hat{H}_T/4$) proved to be acceptable for most jet multiplicities at LO and NLO. The $2j$ case, however, is known to be very sensitive to scale choices, in particular when the minimum jet p_T is fixed (as this constrains significantly the amount of radiation that can be actually emitted from the jets), as verified in our NLO results. For this reason, other possible scales were tested, with a central scale of $\hat{H}_T$ showing a very significant reduction of scale uncertainties. MADGRAPH5_AMC@NLO also provides information on PDF variations, which were found to be negligible compared to scale uncertainties.

Another relevant choice in the study of jet events is the cut in the transverse momentum of the jets. During the course of the project, cross sections were obtained for a range of values of p_T^{min}, going from 20 GeV to 70 GeV. The significance of TPS contributions to the overall cross section (SPS+DPS+TPS) was evaluated for the $6j$ case. These results can be seen in Figures 4 and 5 of Section 4. For the later analysis stage, a p_T^{min}=35 GeV was found to be an appropriate choice.

Cross sections obtained for the study of the pPb case can be calculated based on proton-proton values, as shown in Section 2. For this purpose, pp cross sections were calculated once again, for the energy value corresponding to Heavy-Ion collisions at the LHC, $\sqrt{s} = 8.8$ TeV.

4 Results and Conclusions

Table 1 shows the values of the pp cross sections that were obtained during the project using MADGRAPH5_AMC@NLO, for various jet multiplicities. It also shows the DPS and TPS contributions to $6j$, as calculated according to Section 2.

Table 1: Cross sections for N-jets at LO and NLO accuracy computed with MADGRAPH5_AMC@NLO for pp collisions at $\sqrt{s} = 14$ TeV. All jets are required to have $p_T^j > 35$ GeV and $|\eta^j| < 5$. PDF: NNPDF4.0_LO for LO, and NNPDF4.0_NLO for NLO. Scales: $\hat{H}_T/2$, unless otherwise specified. Jet algorithm: anti-kT (D=0.6). Uncertainties are due to scale variations.

Process	$\sigma^{\rm LO}$	$\sigma^{\rm NLO}$
$pp \to jj$ (SPS) at $\sqrt{s} = 14$ TeV ($\hat{H}_T$)	66.7 μb $^{+28.6\%}_{-21.9\%}$	11.7 μb $^{+95.7\%}_{-205.5\%}$
$pp \to jj$ (SPS) at $\sqrt{s} = 14$ TeV ($\hat{H}_T/2$)	77.9 μb $^{+34\%}_{-25.3\%}$	-7.43 μb $^{+-358.6\%}_{--783.4\%}$
$pp \to 3j$ (SPS) at $\sqrt{s} = 14$ TeV	4.30 μb $^{+38.4\%}_{-26\%}$	3.51 μb $^{+2.7\%}_{-27.2\%}$
$pp \to 4j$ (SPS) at $\sqrt{s} = 14$ TeV	0.71 μb $^{+55.9\%}_{-33.5\%}$	–
$pp \to 4j + 2j$ (DPS) at $\sqrt{s} = 14$ TeV	3157 pb	–
$pp \to 3j + 3j$ (DPS) at $\sqrt{s} = 14$ TeV	616 pb	476 pb
$pp \to 6j$ (TPS) at $\sqrt{s} = 14$ TeV	220 pb	2.08 pb

Some relevant observations can be made from this table. Results for the $2j$ case are compared for scales $\hat{H}_T$ and $\hat{H}_T/2$, showing the aforementioned differences in scale uncertainties, particularly at NLO. It is worth noting as well that the NLO result for $\hat{H}_T/2$ is nonphysical.

The $4j$ related NLO results are missing from the results. This is due to the particular challenges that the Monte Carlo generation of this process posed. Due to the dramatic increase in contributing processes as jet multiplicity increases, $4j$ simulations are computationally demanding, which represented an obstacle for obtaining results within the time-frame of the project.

The corresponding results obtained from the Alpgen generator for the pp case are shown on Table 2. This allow us to verify the compatibility of the $6j$ result provided by Alpgen and those produced by MADGRAPH5_AMC@NLO for lower jet multiplicities.

Table 2: Cross sections for N-jets at LO accuracy computed with Alpgen for pp collisions at $\sqrt{s} = 14$ TeV. All jets are required to have $p_{\mathrm{T}}^{j} > 35$ GeV and $|\eta^{j}| < 5$, and minimum jet separation drjmin = 0.6. Uncertainties are numerical only. Dynamical scale corresponding to $\hat{H}_T/2$ unless stated.

Process	σ^{LO}
$pp \to jj$ (SPS) at $\sqrt{s} = 14$ TeV ($\hat{H}_T$)	73.8 $\pm$ 0.023 μb
$pp \to 3j$ (SPS) at $\sqrt{s} = 14$ TeV	5.05$\pm$ 0.013 μb
$pp \to 4j$ (SPS) at $\sqrt{s} = 14$ TeV	0.92$\pm$ 0.002 μb
$pp \to 6j$ (SPS) at $\sqrt{s} = 14$ TeV	31.5$\pm$ 0.094 nb

Table 3: Cross sections for N-jets at LO and NLO accuracy computed with MadGraph5_aMC@NLO for pp collisions at $\sqrt{s} = 8.8$ TeV. All jets are required to have $p_{\mathrm{T}}^{j} > 35$ GeV and $|\eta^{j}| < 5$. PDF: NNPDF4.0_LO for LO, and NNPDF4.0_NLO for NLO. Scales: $\hat{H}_T/2$, unless otherwise specified. Jet algorithm: anti-kT (D=0.6). Uncertainties are due to scale variations.

Process	σ^{LO}	σ^{NLO}
$pp \to jj$ (SPS) at $\sqrt{s} = 14$ TeV ($\hat{H}_T$)	31.1 μb $^{+25.6\%}_{-19.7\%}$	8.41 μb $^{+73.2\%}_{-140.0\%}$
$pp \to 3j$ (SPS) at $\sqrt{s} = 14$ TeV	1.69 μb $^{+42.1\%}_{-27.7\%}$	1.54 μb $^{1.7\%}_{-27.2\%}$
$pp \to 4j$ (SPS) at $\sqrt{s} = 14$ TeV	235 nb $^{+59.6\%}_{-34.9\%}$	–
$pPb \to 4j + 2j$ (DPS) at $\sqrt{s} = 14$ TeV	323 nb	–
$pPb \to 3j + 3j$ (DPS) at $\sqrt{s} = 14$ TeV	63.2 nb	525 nb
$pPb \to 6j$ (TPS) at $\sqrt{s} = 14$ TeV	59.6 nb	1.18 nb

Table 4: Cross sections for N-jets at LO accuracy computed with Alpgen for pp collisions at $\sqrt{s} = 14$ TeV. All jets are required to have $p_{\mathrm{T}}^{j} > 35$ GeV and $|\eta^{j}| < 5$, and minimum jet separation drjmin = 0.6. Uncertainties are numerical only. Dynamical scale corresponding to $\hat{H}_T/2$ unless stated.

Process	σ^{LO}
$pp \to jj$ (SPS) at $\sqrt{s} = 14$ TeV ($\hat{H}_T$)	34.8 $\pm$ 0.010 μb
$pp \to 3j$ (SPS) at $\sqrt{s} = 14$ TeV	1.93 $\pm$ 0.004 μb
$pp \to 4j$ (SPS) at $\sqrt{s} = 14$ TeV	282 $\pm$ 0.494 nb
$pp \to 6j$ (SPS) at $\sqrt{s} = 14$ TeV	5.56 $\pm$ 0.017 nb

Tables 3 and 4 show MadGraph5_aMC@NLO and Alpgen cross sections used to study proton-lead jet production.

From these results it was possible to compare the contributions to the total cross sections coming from SPS, DPS and TPS processes. Figures 4 and 5 show the fractions of the total cross section coming from each process type for $6j$ production. The plots were obtained from the Alpgen LO results for pp at $\sqrt{s} = 14$ TeV and $\sqrt{s} = 8.8$ TeV.

These results show a higher relevance of TPS and DPS contributions to cross sections in the pPb case compared to pp, which is particularly significant at low p_T.

Using these results as a jumping off point, further analysis is underway, which will leverage the simulated events which were generated in order to gain further insight on TPS interactions. This analysis will, for example, show which parameters have the most significant effects in the rate of TPS processes expected at currently available particle colliders, which would aid the identification and subsequent studies of TPS events.

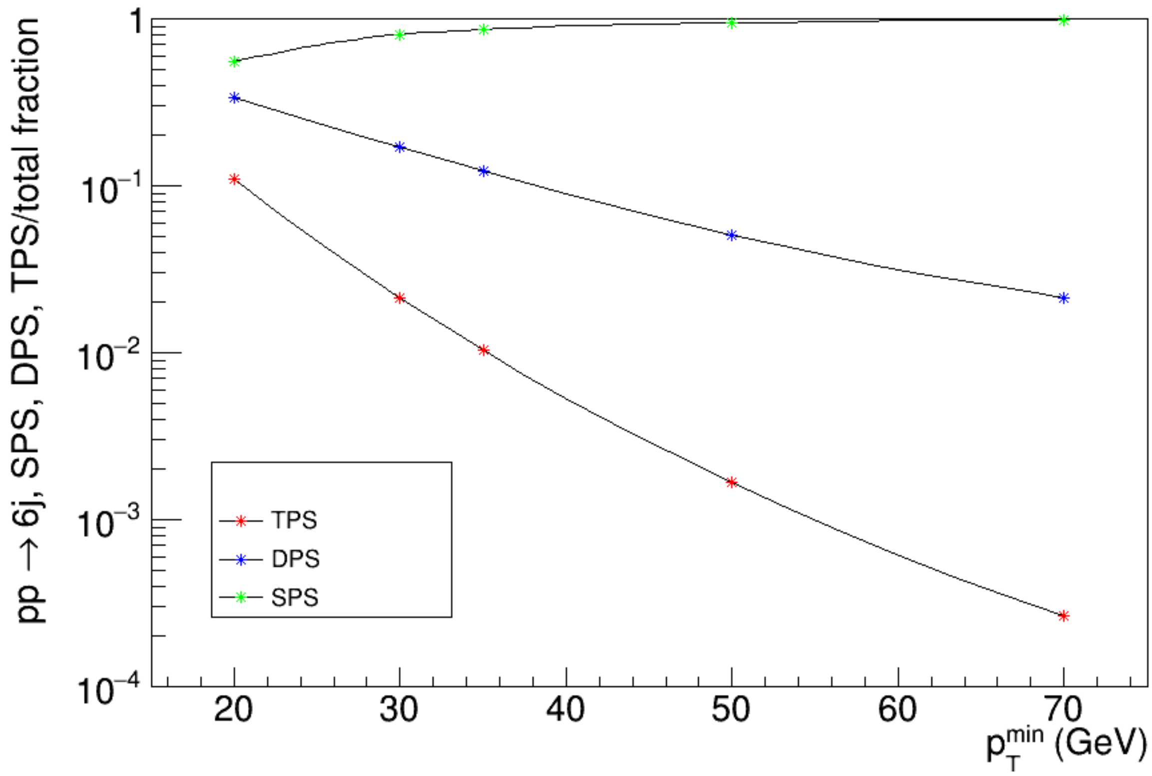

Figure 4: Fractions of total cross section contributions corresponding to TPS, DPS and SPS processes for the $pp \to 6j$ case

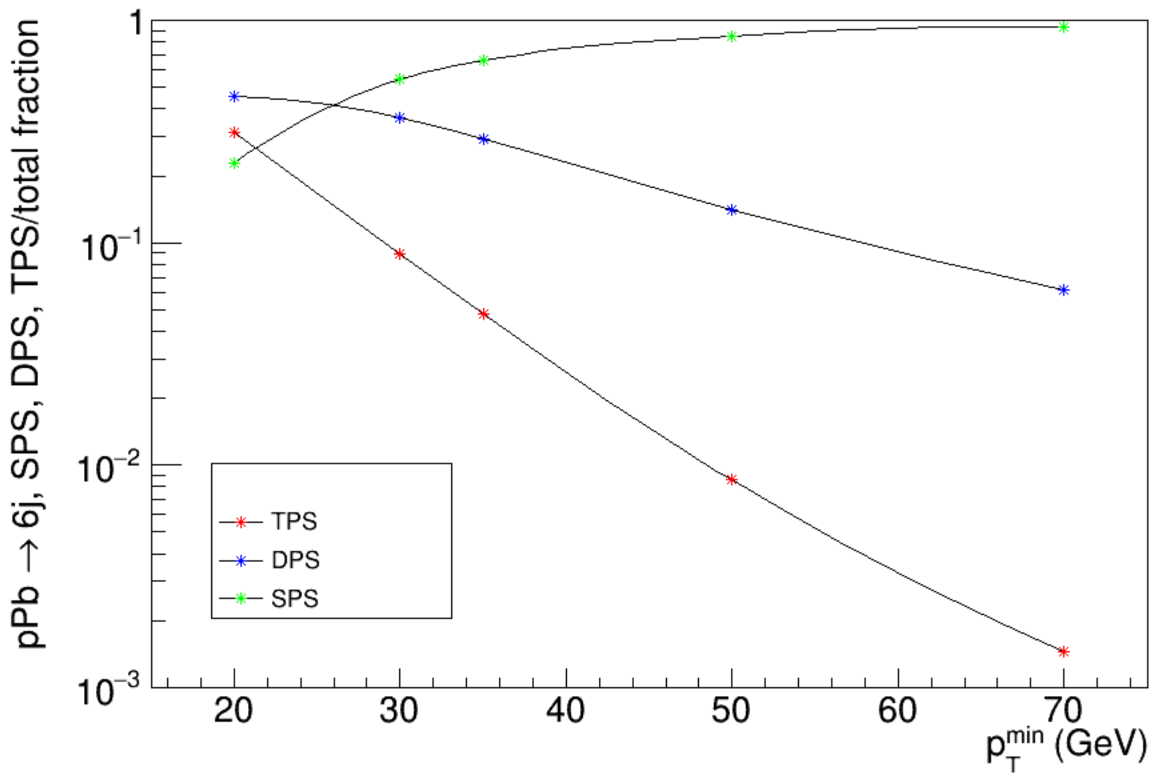

Figure 5: Fractions of total cross section contributions corresponding to TPS, DPS and SPS processes for the $pPb \to 6j$ case

The results will appear in a future publication, with the working title "Six-jet production as a probe of triple parton scatterings at the LHC" (Authors: D. d'Enterria, M. Maneyro).

Bibliography

[1] D. d'Enterria and A. Snigirev, "Double, triple, and n-parton scatterings in high-energy proton and nuclear collisions," *Adv. Ser. Direct. High Energy Phys.* **29** (2018) 159, `arXiv:1708.07519 [hep-ph]`.

[2] D. d'Enterria and A. M. Snigirev, "Triple parton scatterings in high-energy proton-proton collisions," *Phys. Rev. Lett.* **118** (2017) 122001, `arXiv:1612.05582 [hep-ph]`.

[3] **UA2** Collaboration, J. Alitti *et al.*, "A study of multi-jet events at the CERN $\mathrm{p\bar{p}}$ collider and a search for double parton scattering," *Phys. Lett. B* **268** (1991) 145.

[4] **CDF** Collaboration, F. Abe *et al.*, "Study of four jet events and evidence for double parton interactions in $\mathrm{p\bar{p}}$ collisions at $\sqrt{s} = 1.8$ TeV," *Phys. Rev. D* **47** (1993) 4857.

[5] **ATLAS** Collaboration, M. Aaboud *et al.*, "Study of hard double-parton scattering in four-jet events in pp collisions at $\sqrt{s} = 7$ TeV with the ATLAS experiment," *JHEP* **11** (2016) 110, `arXiv:1608.01857 [hep-ex]`.

[6] **CMS** Collaboration, A. Tumasyan *et al.*, "Measurement of double-parton scattering in inclusive production of four jets with low transverse momentum in proton-proton collisions at $\sqrt{s} = 13$ TeV," *JHEP* **01** (2022) 177, `arXiv:2109.13822 [hep-ex]`.